POLISH JOURNAL OF NATURAL SCIENCES
Abbrev.: Pol. J. Natur. Sc., Vol 31(1): 89–99, Y. 2016

VISUALIZATION OF AMARANTH OIL PRESENCE ON THE SURFACE AND INSIDE SPRAY DRIED MICROCAPSULES

***A. Kubiak*[1], *H. Rauscher*[2], *F. Dajnowiec*[1], *P. Banaszczyk*[1], *M. Biegaj*[1], *R. Helminski*[3]**

[1] Faculty of Food Sciences
University of Warmia and Mazury in Olsztyn, Poland
[2] European Commission – Joint Research Centre
Institute for Health and Consumer Protection I-21027 Ispra (VA), Italy
[3] Apostels GmbH, 30827 Garbsen, Heinkelstraße 11, Germany

K e y w o r d s: oil microcapsules, confocal Raman imaging, k-means clustering method.

A b s t r a c t

In order to increase amaranth oil availability to the consumers an encapsulation process by spray drying was applied. Based on the confocal Raman microscopy imaging technique supported by computer image analysis an algorithm for detailed visualization of oil presence on the surface or inside of aggregated microcapsules was performed. Those information are crucial in terms of oil bioavailability as well as storage properties of microcapsules.

WIZUALIZACJA OBECNOŚCI OLEJU Z AMARANTUSA NA POWIERZCHNI I WEWNĄTRZ MIKROKAPSUŁEK OTRZYMANYCH METODĄ SUSZENIA ROZPYŁOWEGO

***A. Kubiak*[1], *H. Rauscher*[2], *F. Dajnowiec*[1], *P. Banaszczyk*[1], *M. Biegaj*[1], *R. Helminski*[3]**

[1] Wydział Nauki o Żywności
Uniwersytet Warmińsko-Mazurski w Olsztynie, Polska
[2] Wspólnotowe Centrum Badawcze Komisji Europejskiej
Instytut Ochrony Zdrowia i Konsumenta I-21027 Ispra (VA), Włochy
[3] Apostels sp. z o. o., 30827 Garbsen, Heinkelstraße 11, Niemcy

S ł o w a k l u c z o w e: mikrokapsułki oleju, konfokalna wizualizacja Ramanowska, klasteryzacja metodą k-średnich.

Address: Aleksander Kubiak, Faculty of Food Sciences, University of Warmia and Mazury in Olsztyn, ul. M. Oczapowskiego 7, 10-719 Olsztyn, Poland, e-mail: aleksander.kubiak@uwm.edu.pl

Abstrakt

W celu podwyższenia dostępności oleju z amarantusa dla jego konsumentów zastosowano proces mikrokapsułkowania poprzez suszenie rozpyłowe. Następnie za pomocą mikroskopu konfokalnego z przystawką do spektrometrii Ramanowskiej oraz komputerowej analizy obrazu przeprowadzono wizualizację oleju znajdującego się zarówno na powierzchni, jak i wewnątrz otrzymanych mikrokapsułek. Informacje te mogą mieć wpływ na biodostępność oleju, jak również na właściwości przechowalnicze mikrokapsułek.

Introduction

The food industry aims at developing new products with functional food properties. This increases the quantity of functional and health promoting ingredients which are delivered to consumers. In order to increase availability of those ingredients to consumers encapsulation process has to be implemented. This process restricts both oxygen migration into the active substances and loss of aromatic compounds and increases resistance to various process-related factors (GOUIN 2004).

Spray drying is a commonly used method of microencapsulation of oil containing materials. The main factors that affect the encapsulation efficiency of microencapsulated oils by spray drying are: type of wall material, properties of the core materials, viscosity, droplet size and process conditions of the spray drying process such as atomization type, inlet air temperature, air flow and humidity (SOLVAL et al. 2012). One of the spray drying limitation is the quantity of material that can be used as a capsule for active ingredients. The compounds used in the process of microencapsulation must be soluble in water. Acacia gum, maltodextrins, modified starch and mixtures thereof, polysaccharides (alginate, carboxymethylcellulose, guar gum) and proteins (whey proteins, soy proteins, sodium caseinate) are widely applied in spray drying technology (FUCHS et al. 2006, GOUIN 2004).

Several techniques can be used to investigate the external and internal structures of microcapsules. Whereas the external size of food microcapsules is in the micrometer range the internal structures of the microcapsules are often in the nanometer range, where objects like pores dimensions and walls thicknesses are smaller than 100 nm, which makes their investigation extremely difficult. A wide range of techniques are available for characterizing food structure, such as: light, fluorescent, transmission and scanning electron microscopy (TIEDE et al. 2008). In order to analyze the outer and inner structure of microcapsules a proper visualization method has to be selected. One of the most popular techniques is the Scanning Electron Microscopy (SEM) (ROSENBERG and SHEU 1996, SOOTTITANTAWAT et al. 2003). The use of an electron microscope gives the opportunity for accurate measurements of the

area and shape of microcapsules and after proper preparation of the sample also the internal structure of microcapsules can be visualized and analyzed (SOOTTITANTAWAT et al. 2003). Despite the huge amount of information which can be collected from the electron microscope image about the size and even size distribution of the pores inside the microcapsule there is still lack of information about the content of microcapsules (DAJNOWIEC et al. 2011). Microcapsules can be empty, or filled with an oil droplet – which is the objective of the encapsulation process. This requires developing a proper methodology of microcapsule assessment, especially with respect to their internal structure.

Raman spectroscopy is an appropriate tool for analysing micro- and macronutrients content in food (LI-CHAN 1996). It allows for a quantitative and qualitative evaluation of tested products based on an analysis of specific spectra which permit the identification of selected bonds between the molecules. Raman spectroscopy has been so far used to determine the composition of products, to control their quality and to detect their eventual adulterations (BATSOULIS et al. 2005).

The aim of this research was evaluation of the applicability of confocal Raman imaging for visualisation of the presence in the internal structure and on the surface of amaranth oil microcapsules.

Material and Methods

The studies were carried out with microcapsules produced under laboratory conditions by spray drying of amaranth oil emulsion. The composition of microencapsulated emulsions were composed of milk protein concentrate MPC with 75% of dry basis 50 g kg^{-1} (ZPM Wolsztyn Ltd. Poland), maltodextrin (DE 7-13%) 100 g kg^{-1}, amaranth oil 200 g kg^{-1} (Szarlat Co. Poland) and water 650 g kg^{-1}. After initial mixing of all ingredients with a mechanical mixer (Zelmer Ltd. Poland), the emulsions were homogenized using a two-stage pressure homogenizer (Nirvo Soavi Panda, Italy). The process was performed at 25/5 MPa on the 1st and the 2nd stage respectively. The spray drying was carried out using a laboratory spray dryer (Anhydro, Denmark). The temperature of the inlet air was 230 ± 6°C and the outlet air was 70 ± 4°C.

Next microcapsules, after cooling in natural conditions, were analyzed in terms of oil presence on its surface and inside. In order to elicit the internal structure microcapsules were deposited on microscopy glass slides or silicon wafers and chopped with a surgical scalpel. Suitable areas of amaranth oil microcapsules were first identified with the optical microscope and then the spectral imaging was performed with a confocal Raman microscope. The instrument used was a Witec alpha 300R with objective 100x, air, NA 0.95;

laser: Spectra Physics Excelsior TEM_{00} single mode Nd:YAG 532 nm and resolution in x-y coordinates (parallel to the sample surface) around 300 nm, in z axis (perpendicular to the sample surface) around 500 nm. Great care was applied to keep the laser power low enough to prevent degradation of the sample over the complete confocal imaging cycle. Raman spectra in the x-y plane as well as along the z-axis were recorded for further analysis of the internal structure of the microcapsules. After identification of the regions characteristic for the main ingredients of investigated microcapsules the Raman spectra were evaluated using the k-means cluster analysis. The goal of the k-means algorithm was to find the best division of n entities (Raman spectra taken for each image pixel) in k=3 groups (the oil droplet, microcapsule's wall and the background), so that the total distance between the group's members x_i^j and its corresponding centroid c_j (average Raman spectrum) representative of the group (or a specific material), is minimized using the following equation:

$$\mathrm{WCSS} = \sum_{j=1}^{k} \sum_{i=1}^{n} \left\| x_i^j - c_j \right\|^2$$

where:
"WCSS" is a within-cluster sum of squares.

Results and Discussion

After inspection of images from an optical microscope two types of structure were identified: smooth oil droplet (Figure 1A) and the microcapsule (Figure 1B). From both of them Raman spectra were obtained. The Raman spectrum of the oil droplet (marked by the cross in the microscope image (Figure 1A) is presented in Figure 2. It can be distinguished from the other structures by a peak at around 1751 cm^{-1} and a distinguishable high intensity peak in the C-H regime at around 2852 cm^{-1}, which is well separated from the other C-H bands. These droplets were the amaranth oil. Figure 3 presents spectra obtained from the surface of the microcapsule marked by the cross on the microscope image Figure 1B.

Thanks to the confocal setup it was possible to obtain distinct Raman spectra of the surface of a microcapsule and from the inside of the microcapsule. The example of the spectrum from inside of the microcapsule (Figure 3B) shows only a very weak peak at 1751 cm^{-1} and a not very well distinguished peak at 2852 cm^{-1}. There is the more pronounced peak at around 482 cm^{-1},

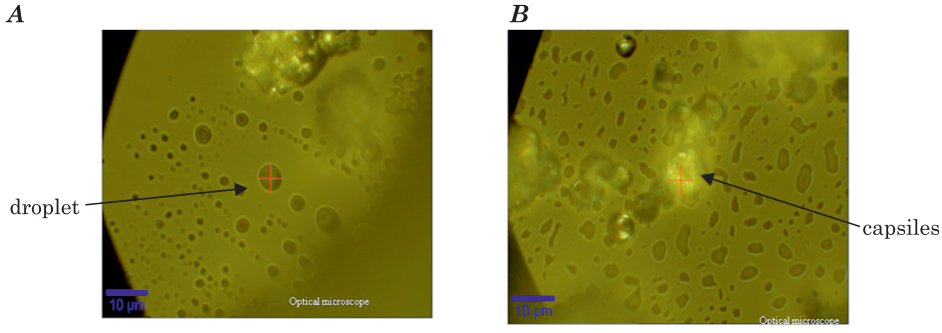

Fig. 1. Oil droplet A) and microcapsule B) visible under confocal microscope

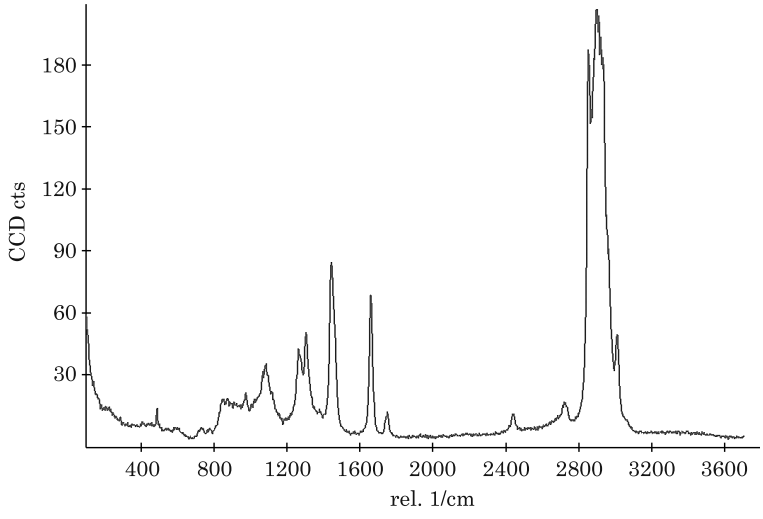

Fig. 2. Raman spectrum of the oil droplet

which is characteristic for the maltodextrin as well as the peaks around 856 cm^{-1} and 940 cm^{-1}.

These three peaks are very weak in the spectrum of the oil droplet (Figure 2). The spectrum obtained from the surface of the microcapsule (Figure 3A) shows also peaks characteristic for maltodextrin and oil. The other peaks cannot be clearly assigned, because they are present in all spectra (however, with different intensity), and probably they are the result of an overlap of the spectra of all three substances (oil, milk protein, maltodextrin). An optical microscope image of another microcapsule is presented in Figure 4A. In order to identify the presence of oil a complete Raman spectrum was made at every pixel in the area marked by a square in the microscope image (60 pixels x 60 pixels=3600 spectra, Figure 4A), and a bandpass filter over the peak at 1751 cm^{-1}

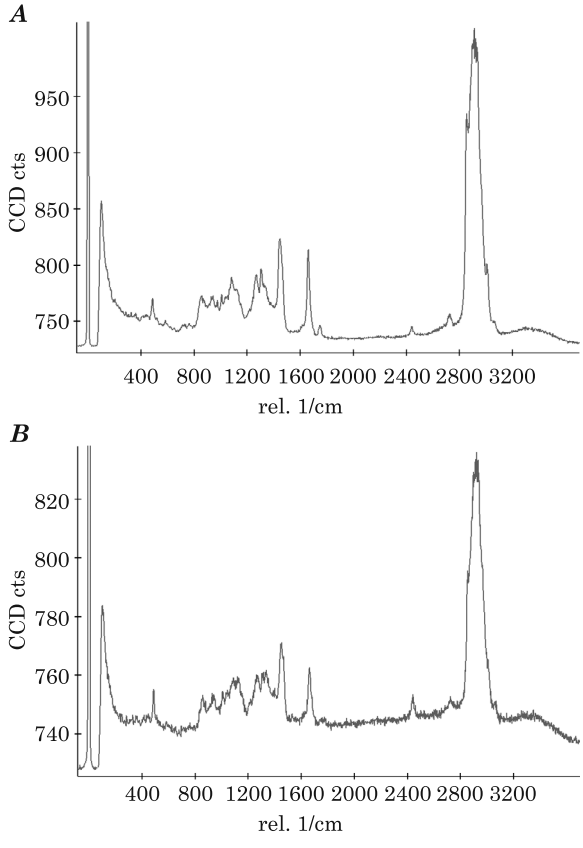

Fig. 3. Raman spectra: A) on the surface of a microcapsule and B) inside a microcapsule

(characteristic for the oil presence Figure 4B) was applied. The result – the intensity of the peak as a function of the position – is displayed in Figure 4C as spectral intensity map. The bright areas on this map show where the oil is present. In this case the oil is visible at the border of the capsule, and there are also two little oil droplets visible on the spectral map – at the top. There are also microcapsules, where oil can be identified inside the microcapsule and such an example is presented in Figure 5. The image under the optical microscope shows a capsule which has a crack probably caused by the scalpel (Figure 5A). Spectral Raman imaging was done within the square marked area and the focal plane was set in the middle of the capsule. A bandpass filter was implemented first for the C-H region between 2828 and 3014 cm^{-1}, and the result is shown in Figure 5B. This image shows all compounds of the capsule i.e., oil, milk protein and maltodextrin, because all these substances have-

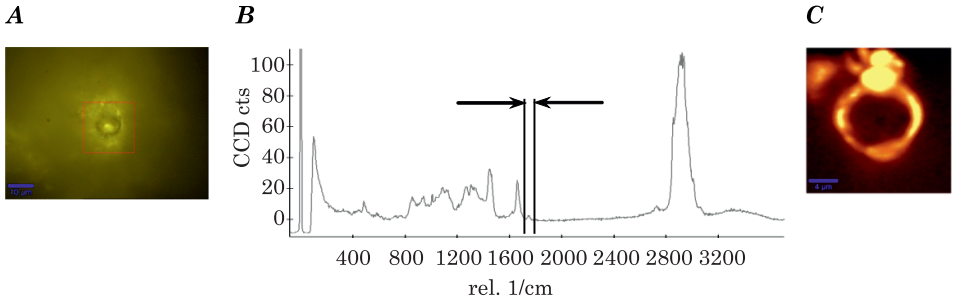

Fig. 4. Single capsule optical microscope image: A) light microscope image with marked analysed square area and the scale bar 10 μm; B) the Raman spectrum with marked region of the bandpass filter implementation; and C) spectral intensity map over the peak at 1751 cm^{-1} within the red square and with the scale bar 4 μm

vibrations in the C-H regime. However, when applying a bandpass filter over the region 1751 cm^{-1} the clear concentration of intensity was visible, which are assigned to the presence of oil.

To gain more information on this issue, a base analysis of the components was made. For this, two regions were identified:

– first region, where the peaks associated with oil at 1751 cm^{-1} and at 2852 cm^{-1} are clearly visible;

– second region, where the 1751 cm^{-1} peak is not visible or is very weak and where the 2852 cm^{-1} peak is not clearly separated, whereas the peak at 482 cm^{-1} demonstrates a high intensit.

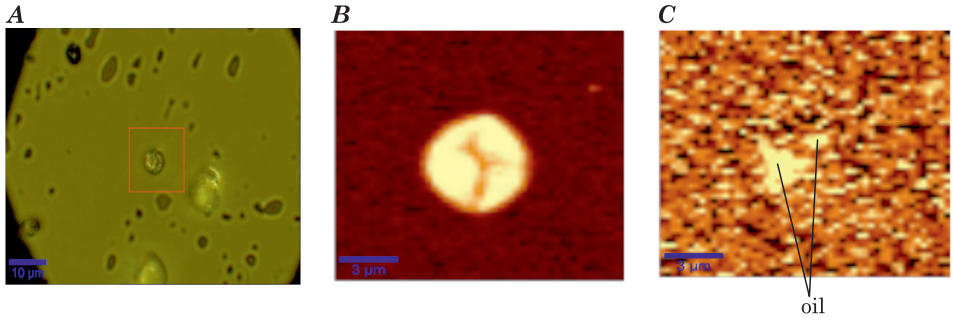

Fig. 5. An image of a single capsule under the optical microscope with marked analysed square area and the scale bar 10 μm (A) and two spectral images after bandpass filtering on the C-H region from 2828 to 3014 cm^{-1} (B) and (C) over the region around the peak 1751 cm^{-1} with a scale bar 3 μm

Average spectra collected in these two regions are displayed in Figure 6A and Figure 6B. As third base spectrum, an average spectrum from the substrate surface (glass) was also collected Figure 6C. These spectra were used as base spectra to fit the measured spectral dataset at every pixel by linear

superposition of the base spectra. As a result, the measured spectra can be very well fitted by this linear superposition, and the obtained weighing factors are displayed as a function of the position in the oil (Region A) and capsule (Region B) of the image presented as a region D in Figure 6D. They are also colour coded and superimposed to obtain the composite image in the region D of Figure 6 together with the substrate spectra region C. The yellow areas in the superposition are characteristic for the presence of oil and the blue for the presence of the capsule material without oil. The substrate is displayed in brown. The location of the oil as obtained from this analysis is in agreement with the result presented on Figure 5C (1751 cm^{-1} peak), although the base analysis shows the distribution of oil in much greater detail.

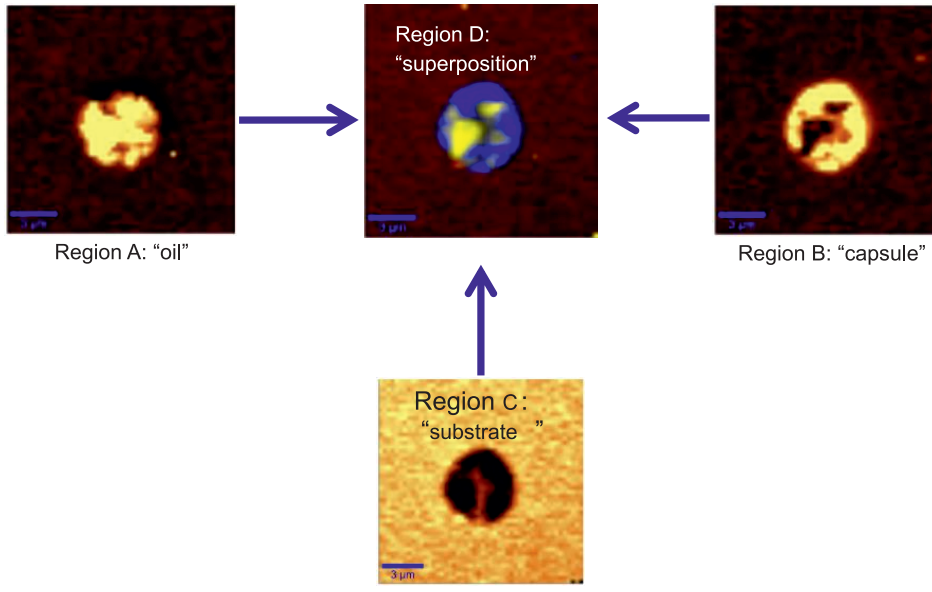

Fig. 6. Single capsule spectral images with the scale bars of 3 μm (description in the text)

For this purpose another aggregated microcapsule was analyzed for which forty complete spectral images were collected at z-distances of 500 nm (i.e., 100 pixels x100 pixels x40=400000 spectra in total). These spectral images were collected using an EMCCD detector, with 10 ms integration time per spectrum. Figure 7 shows selected of these images of the C-H region, obtained at different z-positions, to visualize the overall structure of this microcapsule.

The same microcapsule was used for a more in-depth stochastic analysis of two of these spectral images, obtained at z-positions which are around 1.5 μm apart and shown in Figure 8. In this case, a k-means cluster analysis was performed on the spectral images.

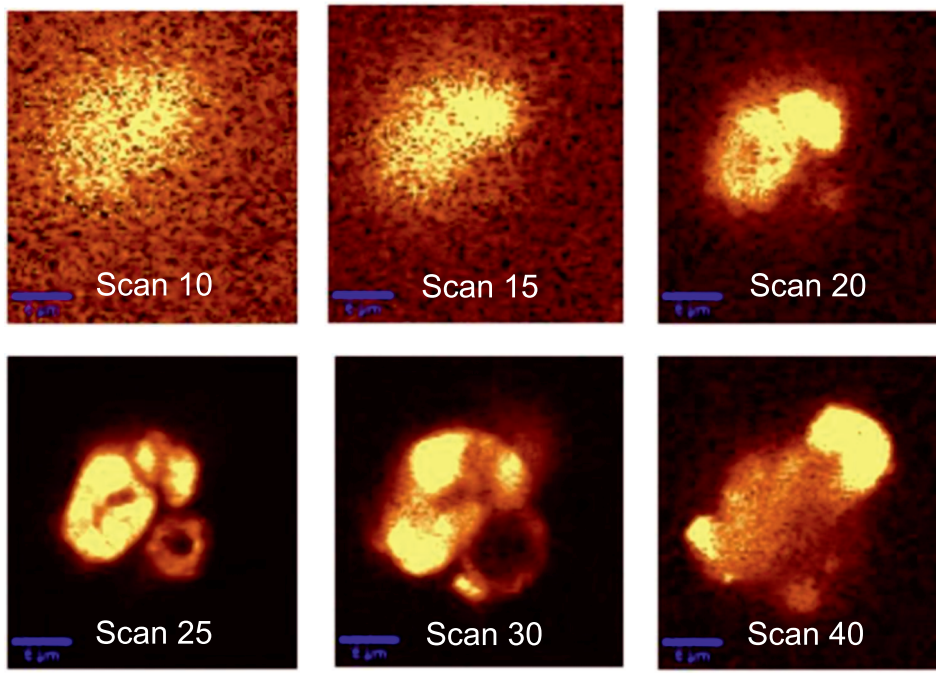

Fig. 7. Example of spectral images of the C-H region obtained at different z-positions for a single capsule (scale bar 6 μm)

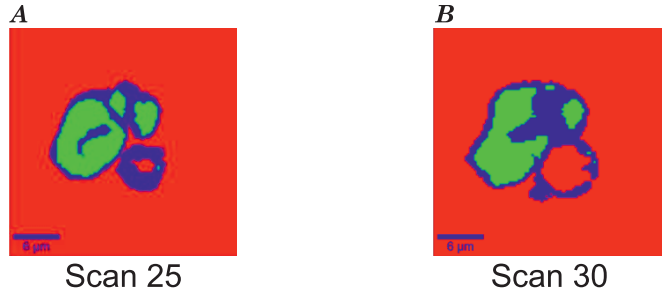

Fig. 8. Examples of images of internal structure of a microcapsule created base on the k-means cluster analysis: B) scan 25 and C) scan 30 (scale bar 6 μm)

Three colour clusters were used to visualize the internal structure of the microcapsule based on the selected Raman spectrums. The red cluster corresponds to the substrate, whereas green and blue clusters are assigned to the capsule. The green cluster corresponds to the oil (see Figure 2) and blue cluster (see Figure 3) corresponds to the capsule materials.

In this case the green areas correspond to a high concentration of oil, i. e., two capsules contain oil, whereas a third one is empty. In the cluster analysis, the cluster spectra oil and the matrix/protein are not as clearly demixed as in the base analysis of the results presented in Figure 6, but nevertheless the two results are compatible with each other and point towards the same conclusion that the oil inside the capsule can be also visualized.

Conclusions

Detailed analysis of the microstructure of the powder particles, based on confocal Raman microscopy imaging supported by computer image analysis, shows that their internal structure can be visualized. Moreover it was revealed that the confocal Raman imaging technique enables identification of particular ingredients and their distribution within the capsules, thus the presence of the surface oil could be detected. The measurements and the analysis are time consuming for routinely microcapsules analysis in the laboratory.

Acknowledgement

This work was supported by the Polish Ministry of Science and Higher Education under Grant number N N312 214539.

Translated by AUTHORS

Accepted for print 4.12.2015

References

BATSOULIS A.N., SIATIS N.G., KIMBARIS A.C., ALISSANDRAKIS E.K., PAPPAS C.S., TARANTILIS P.A. 2005. *FT-Raman spectroscopic simultaneous determination of fructose and glucose in honey*. J Agr. Food Chem., 53(2): 207–210.

DAJNOWIEC F., KUBIAK A., ZANDER L., BANASZCZYK P. 2011. *The structure of microcapsules of ethyl esters of vegetables oils*. Acta Agrophysica, 17(1): 33–41, (in Polish).

FUCHS M., TURCHIULI C., BOHIN M., CUVELIER M.E., ORDONNAUD C., PEYRAT-MAILLARD M.N, DUMOULIN E. 2006. *Encapsulation of oil in powder using spray drying and uidised bed agglomeration*. J Food Eng., 75(1): 27–35.

GOUIN S. 2004. *Microencapsulation: industrial appraisal of existing technologies and trends*. Trends Food Sci. Tech., 15(7–8): 330–347.

JONES P.J., JEW S. 2007. *Functional food development: concept to reality*. Trends Food Sci. Tech., 18(7): 387–390.

KALÁB M., ALLAN-WAJTAS P., MILLER S.S. 1995. *Microscopy and other imaging techniques in food structure analysis*. Trends Food Sci. Tech., 6(6): 177–186.

LI-CHAN E.C.Y. 1996. *The applications of Raman spectroscopy in food science*. Trends Food Sci. Tech., 7(11): 361–370.

ROSENBERG M., SHEU T.Y. 1996. *Microencapsulation of volatiles by spray-drying in whey protein-based wall systems*. Int. Dairy J., 6(3): 273–284.

SOLVAL K.M., SUNDARARAJAN S., ALFARO L., SATHIVEL S. 2012. *Development of cantaloupe (Cucumis melo) juice powders using spray drying technology*. LWT – Food Sci. Technol., 46(1): 287–293.

SOOTTITANTAWAT A.H., YOSHII T., FURUTA M., OHKAWARA P., LINKO P. 2003. *Microencapsulation by Spray Drying: Influence of emulsion size on the retention of volatile compounds*. J Food Sci., 68(7): 2256–2262.

TIEDE K., BOXALL A.B.A., TEAR S.P., LEWIS J., DAVID H., HASSELLÖV M. 2008. *Detection and characterization of engineered nanoparticles in food and the environment*. Food Addit. Contam., 25(7): 795–821.